GATING CURRENTS IN THE INTACT CRAYFISH GIANT AXON

J. G. STARKUS, B. D. FELLMETH, AND M. D. RAYNER, *Department of Physiology, School of Medicine, and Bekesy Laboratory of Neurobiology, University of Hawaii, Honolulu, Hawaii 96822*

ABSTRACT Both single-sweep and signal-averaged asymmetry current are measured from intact crayfish axons after ionic currents are blocked with tetrodotoxin and 4-aminopyridine. The ON asymmetry charge saturates at about 0 mV and no ON charge movement is detectable at voltages negative to −140 mV. The areas of ON and OFF asymmetry charge are equal for short depolarizations but the ratio Q_{OFF}/Q_{ON} decreases for longer depolarizing pulses. Sodium and asymmetry current magnitudes can be changed in parallel by lowering the hold potential or by imposing conditioning prepulses. Our results are consistent with the concept that asymmetry current is generated by movement of trapped charge in association with Na channel gating.

INTRODUCTION

"Gating" currents (Armstrong and Bezanilla, 1973) have been reported from a number of different nerve membrane preparations including, most recently, the crayfish giant axon (Swenson, 1980; 1981). In squid axons (Armstrong and Bezanilla, 1974; Keynes and Rojas, 1974), in vertebrate nodes (Neumcke et al., 1976), and in *Myxicola* giant axons (Bullock and Schauf, 1978; 1979) such asymmetric capacity currents have been shown to be generated by mobile charge trapped within the axon membrane. Additionally, the voltage-dependent behavior of these currents seems related, at least in part, to the molecular mechanism regulating sodium conductance (Almers, 1978; Armstrong and Gilly, 1979). Our results confirm the presence of asymmetric capacity currents in crayfish axons and suggest that these axons may offer certain advantages (see Discussion) over other preparations. Preliminary reports of this investigation have been published (Starkus and Rayner, 1980; Starkus et al., 1981).

METHODS

Preparation

Currents under voltage-clamp conditions were measured using single, nonperfused, medial giant axons (150–300 μm in diameter) dissected from the ventral nerve cord of the crayfish *Procambarus clarkii*. In dissection, mounting of the nerve fiber within the chamber, placement and alignment of the electrodes, and arrangement of the cooling devices, we followed the techniques described by Shrager (1974, 1977). Crayfish were collected locally from freshwater streams on the island of Oahu.

Voltage Clamp

A "piggy-back" axial electrode assembly was inserted longitudinally into the axons. The internal potential monitoring electrode was a 30-μm o.d. glass pipette cemented with lacquer to a current-passing

electrode, which was a 25 μm platinized platinum wire (Shrager, 1974). Membrane currents were measured by the virtual ground method and area compensation was carried out in a circuit similar to that described by Moore and Cole (1963). Series resistance compensation was achieved with a circuit suggested to us by Dr. Begenisich. This circuit (Levis, 1979) allows the additional neutralization of phase-shifts between voltage and current inputs, and permits a more complete compensation of series resistance without the danger that lethal instabilities will develope in the circuit. Transmembrane current (I_m) was tapped from the central 2-mm plate, which was flanked by two 3-mm guard plates. These electrodes were C-shaped to permit a close approach over a greater region of axon surface (Starkus and Shrager, 1978). Clamp speed (20–30 μs) was measured as the time required for the linear capacity transient to settle to a steady-state leakage level (see Fig. 2 *A*) during a control pulse pattern.

We corrected for junction potentials at the difference operational amplifier. Potential drift in the clamp circuit was always <5 mV after 3–5 h of data recording.

Solutions

All experiments were initiated in a standard solution (Van Harreveld, 1936) containing 205 mM NaCl, 5.4 mM KCl, 2.6 mM $MgCl_2$, 13.5 mM $CaCl_2$, 2.3 mM $NaHCO_3$, with pH adjusted to 7.55 by addition of 1 N HCl. When holding at the resting potential of crayfish axons in this solution (−75 to −80 mV), we observed 50–80% steady-state inactivation of both sodium and gating currents. This inactivation could be removed by holding in the range −95 to −105 mV. To hold in this range, external potassium concentration must be decreased from 5.4 to 1.0 mM to keep the holding current low. Low sodium solutions (1/3 or 1/12 the normal sodium concentration by tetramethylammonium [TMA] substitution) were used to permit direct comparisons between gating and ionic currents.

Blockage of Ionic Currents

Tetrodotoxin (Calbiochem Co., La Jolla, Calif.) was used either at 100 or 300 nM for blockade of sodium currents. Effective blockade of potassium conductance was achieved with 0.5 mM 4-aminopyridine (Yeh et al., 1976) obtained from Aldrich Chemical Co., Milwaukee, Wis.; pH was readjusted after this alkaline agent was added to the external perfusing medium. At negative membrane potentials, for pulse durations of <5 ms, no potassium current can be detected in the presence of 0.5 mM 4-aminopyridine; however, some relief of this blockade may develop at large positive membrane potentials in pulses >1 ms. Fortunately (see Fig. 1) the gating current is complete before any detectable

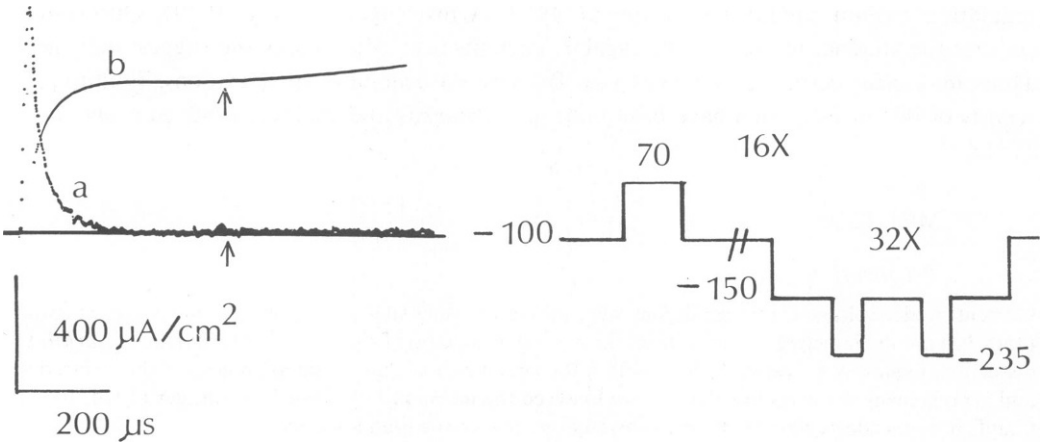

FIGURE 1 Effectiveness of 4AP block on potassium current. (*a*) linear capacity subtracted record in TTX; (*b*) integral of trace (*a*). Arrows indicate approximate time of 4AP relief of potassium block. Solid base line set at steady-state leakage current. Axon 010881: temperature, 5°C; 100 nM TTX; 0.5 mM 4AP; normal Na; 1.0 mM K modified VH solution.

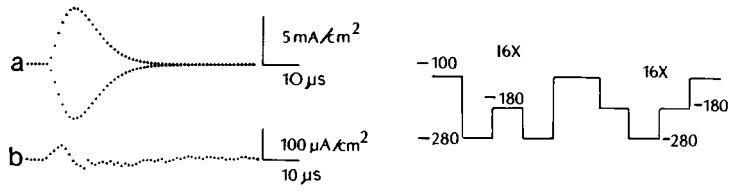

FIGURE 2 Test of the method for elimination of linear capacity current. (*a*) Capacity currents associated with comparable positive and negative pulses from −280 to −180 or −180 to −280 mV respectively (see pulse-pattern insert). (*b*) Small residual signal after subtraction of the capacity currents (note change of gain between *a* and *b*). Traces illustrated were sampled at 1 μs/point and represent an average of 16 traces. Axon 012181: temperature, 5°C; 100 nM TTX; 0.5 mM 4AP; 1/12 Na, 1 mM K; modified Van Harreveld (VH) solution.

relief of potassium block, so that gating charge movements are uncontaminated by potassium currents even at potentials as high as +90 mV. This illustrates the extreme sensitivity of the integration of gating currents as a monitor for even the smallest artifactual currents from such possible sources as potassium relief, membrane breakdown, or electrode polarization. These currents would obscure the flat plateau in the integration records.

With these two externally applied active pharmacological agents, effective block of the ionic currents can be achieved without axoplasmic modification.

Data Recording

Data were collected with two systems. Figs. 10 and 11 show single-sweep records digitized using a Physical Data transient recorder (model 514A, Beaverton, Ore.) with variable gain and a maximum sample rate of 0.5 μs at 10-bit resolution. We did not subtract linear capacity current in these records, because 10-bit precision is inadequate to preserve the entire capacity transient or accurately characterize the relatively small asymmetry current. Pulses were generated by an analog circuit with an accuracy of 2%.

To measure total charge moved and to record the early time-course of the asymmetry current, however, both direct subtraction of linear capacitance and signal averaging are required. In crayfish axons, with their relatively large asymmetry currents, 12-bit resolution permits the entire capacity transient to be digitized with enough resolution remaining to characterize the asymmetry current, provided that command pulses are generated with sufficient accuracy so that control and experimental pulse sizes are precisely matched. In the rest of our work (other than Figs. 10 and 11) we used a Nicolet (Nic) 1170 signal averager equipped with the 172 plug-in digitizer which delivered 12-bit digitization at a 1-μs sample rate. Command pulses were generated by a programmable pulse generator (Adtech, Honolulu, Hi) with 12-bit D/A precision and an accuracy to within 0.2% of the desired voltage. The

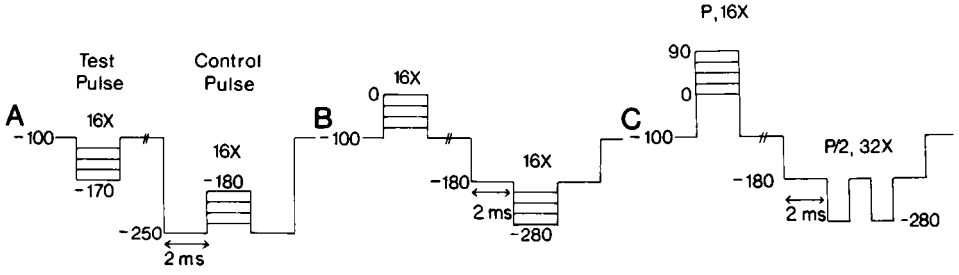

FIGURE 3 Pulse program used for recording gating currents. (*A*) Pulses used for potentials negative to hold. (*B*) Pulse program used for potentials between −100 and 0 mV. (*C*) Divided pulse procedure for potentials between 0 and 90 mV.

successful subtraction of two control pulses is illustrated in Fig. 2. Because of the high clock rate of the digitizer (20 MHz) it was not necessary to synchronize the clocks of the digitizer and pulse generator.

Digital data were stored in the Nic 1170 memory and then transferred directly to an 8-in floppy disk with an Ohio Scientific microcomputer (C3-S1) (Ohio Scientific, Inc., Aurora, Ohio). During analysis, data were retrieved from disk onto the Nic 1170. All integrations were obtained through the processing features of the Nic 1170. Illustrations were made from polaroid pictures of the Nic digital oscilliscope screen.

Elimination of Linear Capacity Currents

Linear capacity transients were eliminated by summing control pulses of opposite polarity to the test pulses (Fig. 3). The control command pulses, generated on the axon, fell within the voltage range -180 to -280 mV. The Q vs. V_m plot indicates asymmetry charge saturation at -120 mV; thus the -180 mV ceiling for control-pulse generation leaves a good margin of safety. The use of this range as a source of control pulses requires that the axon be able to tolerate pulses to -280 mV without membrane breakdown (Armstrong and Bezanilla, 1974) or without any apparent time-dependent inward leakage current (Meves and Vogel, 1977 [Fig. 6]). We looked for these problems in several axons by producing repetitive pulses from -180 to -270 mV for 5 ms before tetrodotoxin (TTX) application. The axons responded with a flat inward leakage current record at -270 mV, and subsequent depolarizing pulses from holding potential showed unchanged sodium and outward steady-state leakage currents. After TTX was applied, gating-current integrations and leak levels remained unchanged during several hours of control pulse generation.

Linear capacity current was thus eliminated by direct summation of the currents associated with test and control pulses from the axon itself. Neither blanking procedures (Armstrong and Bezanilla, 1974) nor capacity transient generator (Bezanilla and Armstrong, 1977) were needed. However, because of the high speed of the clamp and the fast kinetics of crayfish axons, a sampling rate of 1 μs or less was necessary to achieve the detailed characterization of the early time-course of the asymmetry current.

To measure the net charge displacement in the range -150 to $+90$ mV, three pulse programs were used (Fig. 3). The choice depended on the required test-pulse range (i.e., -100 to -170, -100 to 0, and 0 to $+90$ mV). Fig. 3 *A* shows the protocol used for voltages more negative than the holding potential. 16 test pulses to the desired voltage were alternately summed with 16 control pulses of equal magnitude and opposite polarity. The depolarizing control pulses were taken from a base voltage of -250 mV after 2 ms of conditioning. Depolarizing charge movement in the range -100 to 0 mV was measured with the pulse program shown in Fig. 3 *B*. Hyperpolarizing, equal-sized control pulses from -180 mV (again, after 2 ms of conditioning) were alternately summed with depolarizing test pulses. This protocol could not be extended to voltages >0 mV, as the safe control voltage range (-180 to -280 mV) for crayfish axons cannot accommodate control pulses of appropriate size. A divided pulse protocol, $P/2$, (similar to that of Armstrong and Bezanilla, 1974) was used (See Fig. 3 *C*) alternating test and paired control pulses. Charge measurements at 0 mV with full-sized controls ($P/1$) and half-sized controls ($P/2$) were not significantly different.

The stability of crayfish axons at hyperpolarizing voltages (-180 to -280 mV) has been exploited here to minimize nonlinear charge movement associated with control voltage steps and to increase the signal-to-noise ratio by modifying the standard $P/4$ technique (Armstrong and Bezanilla, 1974). When divided control pulses are used, the noise level increases with $\sqrt{n+1}$ where n is the integer divider (i.e., P/n). As noted by Armstrong and Bezanilla (1974 [Fig. 13]), divided control pulses add noise to the signal. Therefore, the best signal-to-noise ratio is achieved by using control pulses as large as the axon will reasonably tolerate, keeping the n integer of the P/n protocol to a minimum.

Leakage Current Subtraction

Because of the nonlinear nature of the steady-state leakage currents in this preparation, we did not attempt to use a linear subtraction method. Corrections for leakage currents were made by defining the steady-state leakage line as zero current in the subtracted data. Integration was then made from this base. This method is feasible because the gating current settled to a stable and clearly defined base line

and the magnitude of leakage current before the pulse was only slightly different from the steady-state pulse level.

Temperature Control

All experiments were run at 5°C, and temperature control was maintained to within ±0.1°C except during solution changes. Regulation was carried out by an electronic feedback circuit connected to two thermoelectric cooling devices (Cambion Corp., Cambridge, Mass.) and to a thermilinear thermistor (YSI 44202, Yellow Springs Instrument Co., Yellow Springs, Ohio).

RESULTS

Characterization of the Asymmetry Current

Fig. 4 compares the current associated with a test depolarization to 0 mV with its corresponding control-pulse current and shows the resulting asymmetry current obtained by elimination of the linear capacity component. Normally these currents are collected by alternating test and control pulses and maintaining a running average of test and control currents together. For this figure, however, test and control currents were alternated but accumulated separately. Fig. 4 *A* shows a low gain superimposition of the test current and the inverted control current. The digitized points (1.0 μs/point) of the two currents nearly overlie on the rising phase but the test current diverges from the control current during the falling phase and subsequent 250 μs.

Fig. 4 *B* shows the same current records except that the first 18 μs on the rising phase have been shifted off the CRO screen, the vertical gain has been increased, the time scale has been compressed, and a straight line has been added to indicate the steady-state leakage current level. This figure emphasizes the diverging sections of the falling phase for the two currents. The test current shows a large, clearly defined residual current that greatly outlasts the linear capacity transient. The control pulse, on the other hand, settles within the 25-μs clamp settling time, leaving a barely discernable residual component. This small current may represent lossy capacitance (Almers, 1978) or a small amount of mobile charge that moved during the control pulse. Fig. 4 *C* shows the asymmetry current at a higher gain after subtracting the control current from the test current. Four possible sources may generate such an asymmetric current: (*a*) differences between the sizes of test and control pulses, (*b*) differences in linear

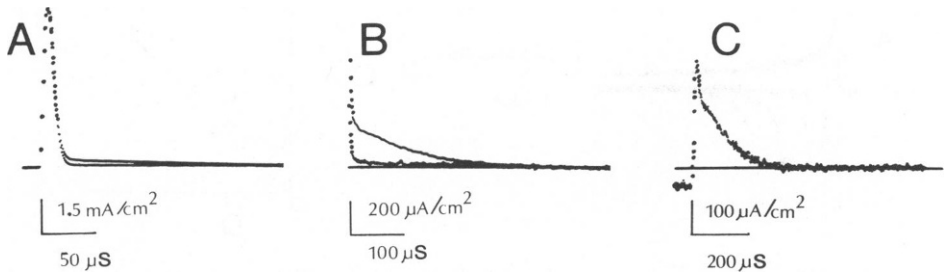

FIGURE 4 Signal-averaged capacity currents associated with test depolarizations to 0 mV and control pulses of equal magnitude. *A*, Superimposition of test and control capacity currents. *B*, The foot of the falling phase for the capacity current transients (see text). *C*, Asymmetry current obtained by subtracting control current from test current. Pulse program as in Fig. 3 *B*, hold potential at −105 mV. Modified VH solution: 100 nM TTX; 0.5 mM 4AP; 1 mM K; normal Na; axon 010881; temperature, 5°C.

membrane capacitance between the test and control voltage ranges, (*c*) a rapidly activating and inactivating TTX-insensitive ionic current, and (*d*) movement of trapped membrane charge.

The first two possibilities would predict an asymmetry current starting from time zero and ending at the clamp charge time (25 μs); this is clearly not the case. Thus, an ionic current or trapped membrane charge remain as possible sources of the asymmetry current.

According to Armstrong and Bezanilla (1974), these possibilities can be distinguished by examining the peak amplitude of inward tails imposed along the falling phase of the asymmetry current. An ionic current would show decreasing tails as the current inactivates, but a current from trapped charge movement would show increasing tails since there would be more charge available to return after longer test-pulse durations. Fig. 5 shows that our results are consistent with the trapped charge interpretation. This concept is also substantiated by our Q/V_m plot, which not only reveals the absence of a reversal potential but also demonstrates saturation of charge movement at positive membrane potentials and at potentials negative to −110 mV (see Fig. 7).

Distribution of Asymmetry Current as a Function of Membrane Voltage

Asymmetry currents and their integrations at various depolarized membrane potentials are illustrated in Fig. 6, where the following points are demonstrated: (*a*) the total charge movement increases up to 0 mV (Fig. 6 *a*, *b*, and *c*) and saturates at positive voltages (Fig. 6 *d* and *e*). (*b*) At least three kinetic components appear in the falling phase of the asymmetry current: an initial fast component, an intermediate component with an apparently linear falling phase, and a slow component. These three distinct kinetic components are especially apparent at positive membrane voltages, a range where the signal is larger and faster, (*c*) The rates of the fast and intermediate components are clearly voltage sensitive; both increase with depolarization. Voltage sensitivity of the slow component (most visible at 20 and 30 mV) is not immediately obvious.

The distribution of charge as a function of membrane potential is shown in Fig. 7. The data from two axons were normalized separately, and the two Q_{max} values were 35.47 and 36.26 nC/cm^2. The midpoint of the distribution lies at −35 mV. The voltage dependence is steepest

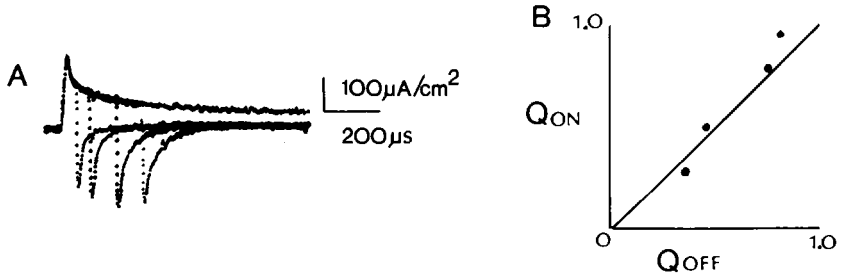

FIGURE 5 Outward ON asymmetry current at −20 mV and inward OFF asymmetry current following return to hold potential after pulse durations of 50, 100, 200 and 300 μs (*A*). For pulse program see Fig. 3 *B*; hold potential, −100 mV. *B*, Outward charge movement plotted against integrated inward current at step-end for the various pulse durations. Axon 012181. External solution: 100 nM TTX, 0.5 mM 4AP, 1 mM K, 1/12 Na-modified VH solution.

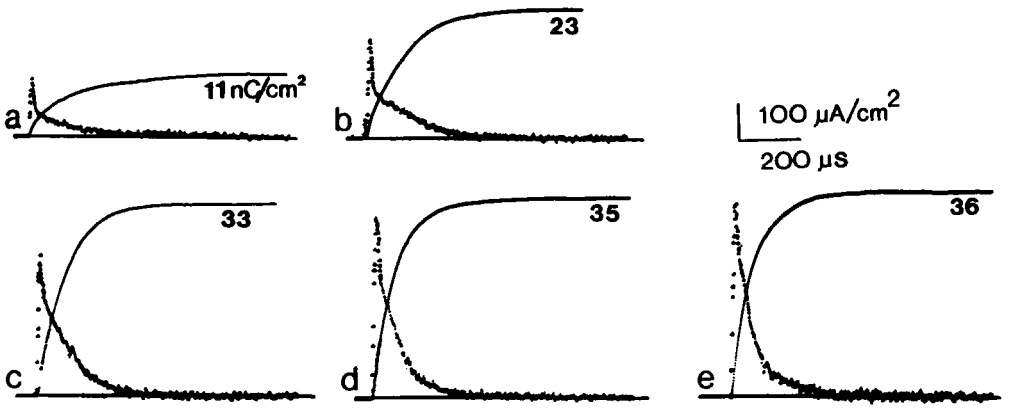

FIGURE 6 Asymmetry current and its integration at various membrane potentials. Base line set at steady state leak. See Fig. 3*B* and *C* for pulse programs; hold potential was −105 mV. Final voltages were (*a*) −40 mV; (*b*) −20 mV; (*c*) 0 mV; (*d*) +20 mV; (*e*) +30 mV. Numbers adjacent to integration records in each panel indicate total charge moved in nC/cm². Axon 010881, 5°C. External solution: 100 nM TTX, 0.5 mM 4AP, 1 mM K, and normal Na-modified VH solution.

between −50 and −10 mV, representing 14 mV for an *e*-fold change, equivalent to an "effective valence" of 1.8 *e*, calculated by the method of Keynes and Rojas (1976).

Effect of Pulse Duration ON the OFF Response

Fig. 8 *a* shows the outward ON asymmetry current at −20 mV and the inward OFF asymmetry current obtained by the return of the pulse to the holding voltage after 10 different

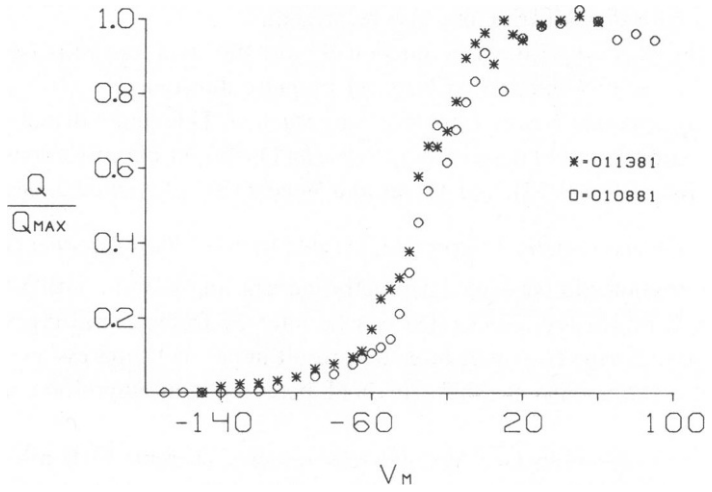

FIGURE 7 Nonlinear charge movement over the voltage range (V_m) of −170 to +90 mV for two axons. Pulse programs as shown in Fig. 3*A, B, C*. Hold potential was −100 mV for axon 011381 and −105 mV for axon 010881; temperature, 5°C. External solution: 100 nM TTX, 0.5 mM 4AP, 1 mM K, and normal Na.

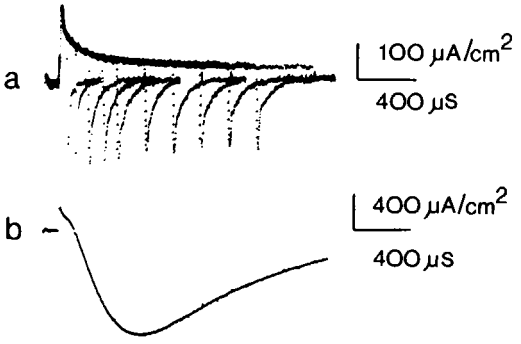

FIGURE 8

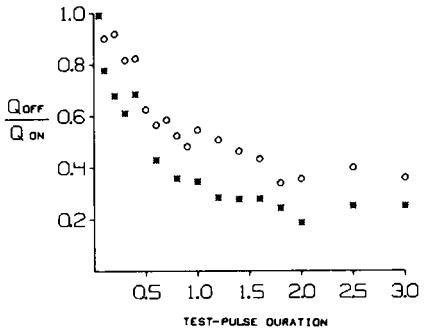

FIGURE 9

FIGURE 8 (*a*) ON asymmetry current for a step to −20 mV from a hold of −100 mV and OFF asymmetry current following pulse durations of 0.05, 0.1, 0.2, 0.3, 0.4, 0.6, 0.8, 1.0, 1.2, 1.4 ms. (*b*) Sodium current at −20 mV before TTX application. Axon 012181, temperature 5°C, 100 nM TTX, 0.5 mM 4AP, 1 mM K, 1/12 Na-modified VH solution.

FIGURE 9 Immobilization of asymmetry current during pulses to −20 (○) and 0 (*) mV from a hold potential of −100 mV. The OFF:ON ratio is near 1.0 for short durations but falls to 0.4 for −20 mV and 0.3 for 0 mV at times longer than 2 ms. Axon 012181, temperature 5°C. External solution: 100 nM TTX, 0.5 mM 4AP, 1/12 Na, 1 mM K-modified VH solution. Test-pulse duration is expressed in milliseconds.

pulse durations. Fig. 8 *b* shows the inward sodium current plus the outward asymmetry current at the same voltage before TTX was added.

During the falling phase of the OFF asymmetry currents, two kinetic components are apparent. The first is a very fast component with kinetics resembling the fast ON component seen in Fig. 6. The second component decays with an intermediate rate. Unlike the very fast component, its rate clearly decreases as the duration of the depolarizing pulse is increased. A third component with slow kinetics may also be present.

Fig. 9 shows the Q_{OFF}/Q_{ON} ratio as a function of pulse duration for test pulses to −20 and 0 mV. The limits of the ON integration were set by pulse duration; the OFF integration was continued until an apparent steady-state level was reached. This figure demonstrates "charge immobilization" similar to that described by Swenson (1980) for crayfish axons and earlier by Armstrong and Bezanilla (1977), and Meves and Vogel (1977) for squid axons.

Is Crayfish Asymmetry Current Associated with Sodium Channel Gating?

A direct causal relationship between asymmetry current and sodium gating has never been reported, although an indirect connection can be inferred from several types of correlative evidence. Here we describe two procedures that result in parallel suppression and recovery of asymmetry and sodium current: shifts in hold potential and imposition of conditioning prepulses.

Fig. 10 shows single-sweep (see Methods) asymmetry currents at 0 mV from holds of −100, −85, and −65 mV. Holding at −65 mV resulted in almost total suppression of the ON charge movement, whereas the current from −85 is about half inactivated. The asymmetry and sodium currents resulting from a depolarization to 0 mV from a holding potential of −70 mV are shown in traces *ii* and *iva*, respectively. Both have been substantially inactivated. However, both currents recover to nearly full size in a parallel fashion after a 350 ms

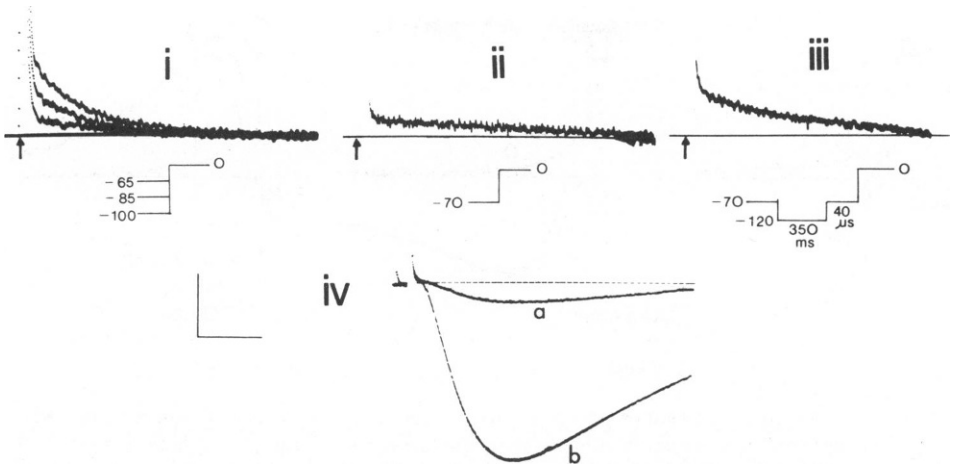

FIGURE 10 Effect of holding potential on single-sweep records of asymmetry currents and sodium current. Onset of the voltage step indicated by an arrow. Base line positioned over steady-state leak levels. (*i*) Asymmetry current associated with steps to 0 mV from holding potentials of −100, −85, and −65 mV. (*ii* and *iva*) Inactivation of asymmetry and sodium currents associated with a step to 0 mV from a hold of −70 mV. (*iii* and *ivb*) Recovery of asymmetry current and sodium current from inactivation after a hyperpolarizing prepulse (see pulse insert). Horizontal scale bar is 200 μs in all records. Vertical scale is 200 $\mu A/cm^2$ in frame *i*, 160 mA/cm^2 in frames *ii* and *iii*, and 2 mA/cm^2 in frame *iv*. Frames *i, ii, iii:* axon 030680 in 300 nM TTX, 0.5 mM 4AP, 1 mM K, 1/3 Na-modified VH solution. Frame *iv:* axon 031380 in normal VH solution (full Na, 5.4 mM K) plus 0.5 mM 4AP without TTX. All records at 5°C.

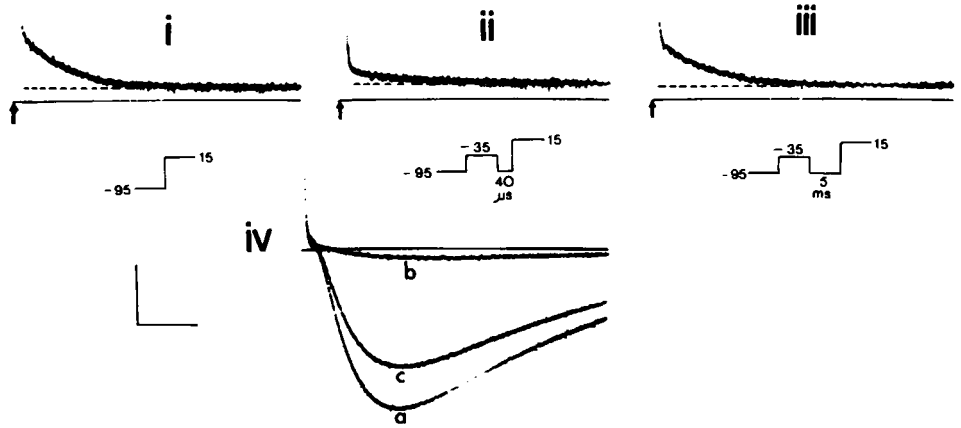

FIGURE 11 Effect of depolarizing prepulses on asymmetry and sodium current. Onset of voltage pulse marked by arrow, leak level by dashed line and holding current level by solid line. (*i* and *iva*) currents for a test pulse from −95 to 15 mV, (*ii* and *ivb*) Reduction of both currents by interposing a depolarizing prepulse to −35 mV for 50 ms, see pulse-pattern insert. (*iii* and *ivc*) Recovery of both currents by increasing the pulse interval from 40 μs to 5 ms. Horizontal scale bar is 200 μs in all records. Vertical bar is 200 $\mu A/cm^2$ in frames *i, ii, iii* and 1 mA/cm^2 in frame *iv*. Frames *i, ii, iii* : axon 030680 in 300 nM TTX, 0.5 mM 4AP, 1 mM K, 1/3 sodium. Frame *iv* : axon 031380 in 0.5 mM 4AP, 1/3 sodium, 1 mM K without TTX. All records at 5°C.

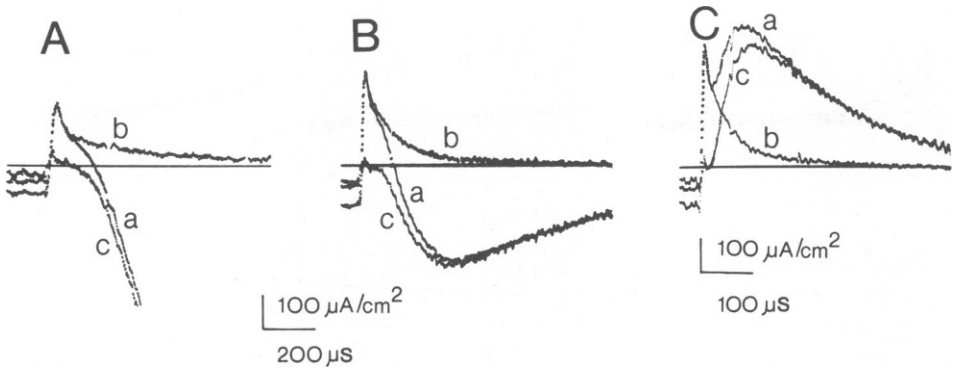

FIGURE 12 Temporal relationship between asymmetry current and activation of sodium current from signal-averaged and linear-capacity current subtracted data at three different membrane potentials: *A*, −20 mV; *B*, 10 mV; *C*, 20 mV. Each panel contains three traces: (*a*) currents (asymmetry and Na) in presence of 4AP; (*b*) asymmetry current after addition of 100 nM TTX; (*c*) pure sodium current obtained by subtraction of *b* from *a*. Straight line indicates steady-state leak level. Axon 012181 in 1/12 sodium, 0.5 mM 4AP, 1 mM K modified VH. Temperature, 5°C.

hyperpolarizing prepulse to −120 (traces *iii* and *ivb*). This result is consistent with the idea of a parallel recovery from the steady-state inactivation induced by a holding potential of −70 mV. Similar parallel behavior is seen when the sodium current is inactivated with a depolarizing prepulse, as illustrated in Fig. 11.

If the asymmetry current is indeed related to Na gating, then one would expect to see a relationship in their time-course and voltage dependence. Fig. 12 compares signal-averaged asymmetry current and sodium current at three voltages. The pure sodium current record (trace *c*) shows an apparent delay before the rapid activation of sodium conductance, and this delay period (trace *c*) correlates with the apparent termination of the fast component of gating current (trace *b*). The rates for both the intermediate component of gating current and sodium activation show parallel voltage dependence; these two currents seem to have similar time-courses. Note that sodium currents generated close to E_{Na} are significantly contaminated by the asymmetry currents.

The data of Figs. 10 and 11 demonstrate parallel inactivation behavior for the asymmetry and sodium currents. Fig. 12 documents the temporal relationship between two of the asymmetry components and sodium activation. These relationships may, of course, be purely coincidental, but the more direct conclusion is that asymmetry charge movement participates in the control of sodium gating in the crayfish axon as has been assumed for other preparations (e.g. squid, frog node, *Myxicola*, see Introduction).

DISCUSSION

Components of Gating Current

The ON gating current apparently contains three components on the falling phase: fast, intermediate, and slow (see Fig. 6 *d* and *e*). The OFF gating current records contain fast and intermediate components and presumably a third component with such slow kinetics that it is difficult to measure. The presence of an unmeasurably slow OFF component may be inferred

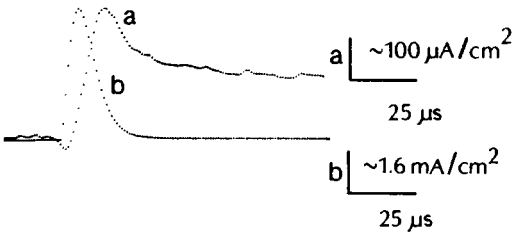

FIGURE 13 Temporal separation of gating current (*a*) and control capacity current (*b*) at −25 mV. Hold potential, −100 mV. Pulse pattern as in Fig. 3 *B*. Temperature, 5°C. Time scale is the same for each trace. Vertical gains adjusted to match peak heights; approximate gains are indicated.

in order to account for conservation of trapped charge at pulse durations >~200 μs (at −20 mV).

Of the three ON components, the fast component is the only one that cannot be seen without subtraction of linear capacity transients. This component is probably not an artifact either of pulse size mismatch between the control and test pulses or voltage dependence of static membrane capacity (Almers, 1978) because its behavior does not parallel that of the linear capacity current (see Fig. 13).

Both the intermediate component and the slow component occur predominately after the clamp has settled and can thus be well characterized from signal-averaged traces without linear capacity current subtraction (Fig. 4 *B*). Although signal averaging is required to characterize the slow component, the intermediate component is large enough to be measurable even without signal averaging (Figs. 10 and 11). The intermediate component represents the majority of the charge moved and covaries with sodium pore opening. The slow component, although visible at positive membrane potentials, is more difficult to observe at negative potentials because of its very slow time constant in that voltage range. Noting the different properties of these three gating current components, we conclude that they may represent either three separate gating particles or, alternatively, a single particle moving through a complex state array.

Finally, we may ask whether the rising phase of the gating current measured in these axons represents a true kinetic delay as suggested by Armstrong and Gilly (1979). Because the rising phase of the gating current (just 20 μs) does not outlast the voltage-clamp rising phase (20–30 μs), we find no evidence of a true kinetic rising phase even at high membrane depolarizations. We suggest, rather, that the short (6 μs) delay in rise of asymmetry current (see Fig. 13) primarily reflects the nonlinearity of the overall Q/V_m distribution.

Size of the Gating Currents

Gating current magnitude depends, as noted by Almers (1978), on three factors: (*a*) The number and valence of gating charges at each pore, (*b*) the kinetics of gating charge movement, and (*c*) the pore density. The maximum amount of charge moved in crayfish axon is 2,200 electron charges/μm^2, almost twice the 1,300 most recently reported for squid axons (Armstrong and Gilly, 1979).

The larger gating currents arise partly from approximately fourfold faster kinetics of crayfish axon compared with squid. Because the Q/V_m distribution is not strikingly steeper for

crayfish than for squid, indicating a similar charge number per channel, the remainder may well be accounted for by a higher sodium pore density in the crayfish axons. This conclusion is consistent with the 1.7-fold difference in total charge movement noted here. The large size of these currents makes the crayfish giant axon an especially favorable preparation for future detailed work on the relationship between gating and ionic currents.

Q/V_m Distribution

The major contribution to the Q/V_m distribution in Fig. 7 is the intermediate component. The slope is very steep, with 80% of the charge transfer occuring in the range -50 to 0 mV. Although one can compute an "effective valence" for the trapped charge from the slope of the Q/V_m distribution (Keynes and Rojas, 1974; 1976), in our case this distribution is apparently an amalgam of at least three, possibly highly interactive, asymmetry charge components. Any such valence estimate would therefore be difficult to interpret in terms of physical mechanism.

Advantages and Disadvantages of the Crayfish Axon Preparation

There are several advantages to measuring gating currents from crayfish axons despite the high digitization rates necessitated by their fast kinetics. First, we have shown that the major gating component can be measured on single sweeps, thus permitting qualitative studies of gating current without time consuming averaging. Second, the crayfish axon can be held at negative membrane potentials (-100 mV by lowering external potassium concentration from 5 to 1 mM) where resting inactivation has been maximally removed, while large hyperpolarizing control pulses may be imposed without the dangers of introducing membrane breakdown. Third, 4-aminopyridine is a more effective blocking agent in crayfish than in squid. Because of the rapid crayfish gating current kinetics, no relief of K block is observed before the settling of the gating current. It is thus possible to block K currents without resorting to internal perfusion, which may itself distort the true characterization of the gating current by introducing foreign intracellular ions. A comparison of gating currents from the intact and perfused fiber will be necessary to evaluate this possible complication. Finally, the large size of the gating currents may provide better signal-to-noise ratios than are possible in other preparations, yielding more precise separation of kinetic components as well as a more accurate comparison with ionic current kinetics.

The authors are indebted to Dr. Ian Cooke for allowing us to use the Pacific Biological Research Center facilities (Bekesy Lab) and to Dr. D'Arrigo for the loan of his analog oscilloscope (purchased under National Science Foundation grant BNS76-02647). Technical, secretarial, and art assistance from Denise Starkus are greatly appreciated.

Our work was supported in part by the National Institutes of Health (National Institute of Environmental Health Services) Post Doctoral award 1F32-ESO5065-03 to J. G. Starkus, NIH grant GM29263-01 to M. D. Rayner, and Biological Research Support Grant (BRSG) RR05599-13 (University of Hawaii Medical School).

Received for publication 15 April 1980 and in revised form 25 March 1981.

REFERENCES

Almers, W. 1978. Gating currents and charge movements in excitable membranes. *Rev. Physiol. Biochem. Pharmacol.* 82:97–190.

Armstrong, C. M., and F. Bezanilla. 1973. Currents related to the movement of gating particles of the sodium channels. *Nature (Lond.)* 242:459–461.

Armstrong, C. M., and F. Bezanilla. 1974. Charge movement associated with the opening and closing of the activation gates of the Na channels. *J. Gen. Physiol.* 63:533–552.

Armstrong, C. M., and F. Bezanilla. 1977. Inactivation of the sodium channel. II. gating current experiments. *J. Gen. Physiol.* 70:567–590.

Armstrong, C. M., and W. F. Gilly. 1979. Fast and slow steps in the activation of sodium channels. *J. Gen. Physiol.* 74:691–711.

Bezanilla, F., and C. M. Armstrong. 1977. Inactivation of the sodium channel. I. Sodium current experiments. *J. Gen. Physiol.* 70:549–566.

Bullock, J. O., and C. L. Schauf. 1978. Combined voltage clamp and dialysis of Myxicola axons: behavior of membrane asymmetry currents. *J. Physiol. (Lond.)* 278:309–324.

Bullock, J. O., and C. L. Schauf. 1979. Immobilization of intramembrane charge in Myxicola giant axons. *J. Physiol. (Lond.).* 286:157–171.

Keynes, R. D., and E. Rojas. 1974. Kinetics and steady state properties of the charged system controlling sodium conductance in the squid giant axon. *J. Physiol. (Lond.).* 239:393–434.

Keynes, R. D., and E. Rojas. 1976. The temporal and steady state relationships between activation of the sodium conductance and movement of the gating particles in the squid giant axon. *J. Physiol. (Lond.)* 255:157–189.

Levis, R. 1979. Temporal control of potential in a giant axon voltage clamp. *Biophys. J.* 25:306*a*.

Meves, H., and W. Vogel. 1977. Inactivation of the asymmetrical displacement current in giant axon of *Loligo forbesi*. *J. Physiol. (Lond.)* 267:377–393.

Moore, J. W., and K. S. Cole. 1963. Voltage clamp techniques. *In* Physical Techniques in Biological Research. W. L. Nastuk, editor. Academic Press, Inc., New York 5:263–321.

Neumcke, B., W. Nonner, and R. Stampfli. 1976. Asymmetrical displacement current and its relation with the activation of sodium current in the membrane of frog myelinated nerve. *Pflug. Arch. Eur. J. Physiol.* 363:193–203.

Shrager, P. 1974. Ionic conductance changes in voltage clamped crayfish axons at low pH. *J. Gen. Physiol.* 64:666–690.

Shrager, P. 1977. Slow sodium inactivation in nerve after exposure to sulfhydryl blocking reagents. *J. Gen. Physiol.* 69:183–202.

Starkus, J. G., B. D. Fellmeth, and M. D. Rayner. 1981. Gating current from crayfish giant axon. *Biophys. J.* 33:281*a*.

Starkus, J. G., and M. D. Rayner. 1980. Crayfish giant axon. I. Interaction between gating current and sodium inactivation. *Fed. Proc.* 39(6):2420.

Starkus, J. G., and P. Shrager. 1978. Modification of slow sodium inactivation in nerve after internal perfusion with trypsin. *Am. J. Physiol.* 4:C238–244.

Swenson, R. P. 1980. Gating charge immobilization and sodium current inactivation in internally perfused crayfish axon. *Nature (Lond.).* 287:644–645.

Swenson, R. P. 1981. Crayfish gating currents support a coupled model of sodium activation and inactivation. *Biophys. J.* 33:280a.

Van Harreveld, A. 1936. A physiological solution for fresh water crustaceans. *Proc. Soc. Exp. Biol. Med.* 34:428–432.

Yeh, J. Z., G. S. Oxford, C. H. Wu, and T. Narahashi. 1976. Dynamics of amino-pyridine block of potassium channels in squid axon membrane. *J. Gen. Physiol.* 68:519–535.